SOUND PROPAGATION OVER AN ISOLATED SEAMOUNT OFF THE CANADIAN WEST COAST

Gordon R. Ebbeson and N. Ross Chapman

Defence Research Establishment Pacific
Forces Mail Office
Victoria, B.C. VOS 1BO

ABSTRACT

Acoustic shadowing, reflection, and enhancement near an isolated seamount have been studied by examining the results of an experiment carried out to measure the propagation loss over Dickins Seamount off the Canadian west coast. Two types of sound sources were used: a 230-Hz cw projector towed at depths of 18 and 184 m; and 0.82-kg explosives detonated at depths of 24 and 196 m. The receiving system had hydrophones spaced in depth from 329 to 633 m. In the acoustic shadow region, the propagation loss for the shallow sources increased by 15 dB over the loss measured in the absence of the seamount. Examination of the multipath propagation loss for the shots revealed that the received signals consisted of two arrivals. The first and dominant pulse was determined to be a diffracted wave while the subsequent group of weaker pulses was attributed to a series of bottom and surface reflections. Strong reflections from the seamount were observed when the shallow cw source was 3 to 5 km from the seamount peak. For source positions closer to the peak, these reflections changed to downslope reflections resulting in an enhancement of the directly received energy. Only minimal effects were observed in the results for the deep sources because most of the source energy propagated along the sound-channel axis above the seamount peak.

SOMMAIRE

Une expérience, qui avait pour but de mesurer les pertes obtenues lorsqu'il y a propagation au-dessus d'un mont de Dickins, a été réalisée au large des côtes canadiennes. L'ombrage, la réflexion et l'amplification acoustique créés au voisinage d'un mont sous-marin ont été étudiés. Deux types de sources sonores ont été utilisées: un projecteur d'une fréquence de 230 Hz remorqué à des profondeurs de 18 et 184 m, ainsi que 0.82 Kg d'explosif déclanché à des profondeurs de 24 et 196 m. La réception des signaux était assurée par un groupe d'hydrophones disposés sur un axe vertical à des profondeurs variant de 329 à 633 m. Dans la région d'ombrage acoustique, les pertes de propagation sont augmentées de 15 dB comparativement aux pertes mesurées en absence de mont sous-marin. Un examen plus attentif a révélé que le signal reçu était composé de deux groupes de signaux ayant des temps d'arrivée différents. Le premier groupe reçu a été attribué à l'onde diffractée, tandis que le second groupe, constitué d'impulsions plus faibles, a été

expliqué par les réflexions sur le fond et à la surface de l'eau.
De fortes réflexions, introduites par le mont sous-marin, ont été
observées lorsque la source était située de 3 à 5 km du sommet.
Pour des distances inférieures, ces réflexions se réorientent
partiellement vers le fond pour finalement s'ajouter aux ondes
suivant le parcours direct. De faibles effets ont été observés dans
le cas des sources en eau profonde dû au fait que l'énergie se
propage le long de l'axe situé au-dessus du sommet.

INTRODUCTION

Acoustic propagation over an isolated seamount has been studied to
determine how the seamount interacts with the propagating acoustic energy, as
well as how these interactions vary with the depths of the sound source and
receiver, and the position of the source with respect to the seamount and
receiver.[1,2] A series of experiments was carried out over Dickins Seamount
which is located at 54°32'N, 136°55.5'W as shown in Figure 1. Unlike previous
investigations,[3-9] the present propagation loss measurements were made using
both a 230-Hz cw source and small explosive charges at ranges relatively close
to the seamount. With the detailed knowledge of the bathymetry that was
available and the lack of interference from other seamounts, it was possible
to perform a very detailed study of the seamount shadowing effect. These
features also made it possible to extend the study to include an investigation
of the reflection of the source energy from the seamount and the closely
related downslope reflection enhancement.

DESCRIPTION OF THE EXPERIMENT

The configuration of the source tracks with respect to the receiving
system and Dickins Seamount is shown in Figure 2. A continuous-wave (cw)
source with a frequency of 230 Hz was towed at depths of 18 and 184 m. Tracks
1 and 4 were radial runs during which the source was towed over the seamount
at the shallow and deep depths, respectively, out to ranges of between 120 and
130 km. Track 2 was a radial run during which the source, towed at the
shallow depth, traversed 45 km of relatively flat bottom to the east of the
seamount. In addition, 0.82-kg explosives were deployed at average depths of
24 and 196 m at intervals of 1.8 km along track 5 out to a range of 130 km.
The receiving system, which was at a range of 60 km (about 1.5 convergence
zones) from the seamount, consisted of a vertical line array of eight
omnidirectional hydrophones spaced in depth from 329 to 633 m.

The average seamount slope along the tracks was approximately 14° and the
minimum depth near the peak was 420 m. A number of sound-speed profile
measurements were made along the tracks of Figure 2 during the propagation
experiments. The average of these profiles is shown in Figure 3. As is
characteristic of this region of the Northeast Pacific, the profile has two
sound channels. The upper or secondary sound channel has an axis at a depth
of about 95 m while the axis of the lower or deep sound channel is near 300 m.
It is important to note that the deep sound channel axis was shallower than
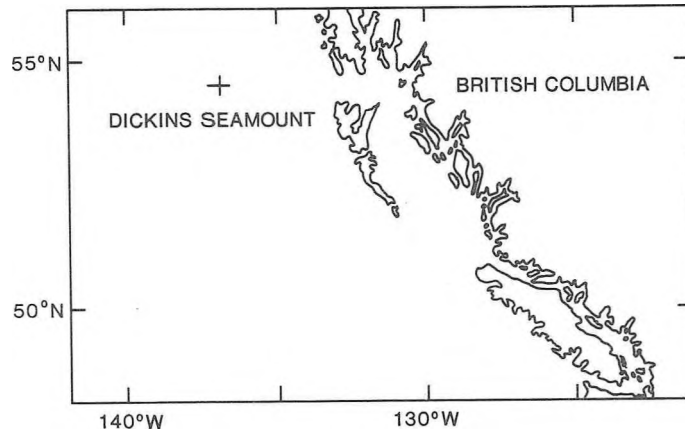the seamount peak.

Figure 1. Location of Dickins Seamount (54°32'N, 136°55.5'W) in the Northeast Pacific Ocean.
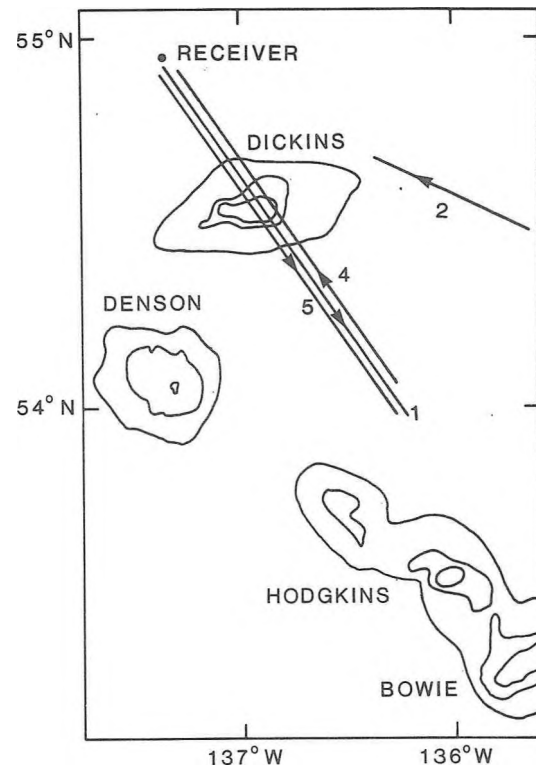
Figure 2. Orientation of the source tracks with respect to the receiver and Dickins Seamount. The depth contours are 1000, 2000, and 3000 m. For tracks 1, 2 and 4 a cw source was used while explosive charges were used for track 5.

ACOUSTIC SHADOWING BY THE SEAMOUNT

The geometry of these propagation loss experiments was designed so that the deep-cycling energy from the sources would, at some point along the runs, be blocked by the seamount. Although the receiver was effectively in an acoustic shadow during this blockage, some energy was still received. Ray theory predicts that the deep-cycling rays propagated over the seamount by a number of bottom-surface reflections up and then down the slope. Diffraction theory, however, predicts that the deep-cycling energy propagated over the seamount by forward scattering from the rough surface of the seamount slope and diffraction over the peak. These mechanisms are discussed in the following sections with an analysis of the measured results to determine which was the dominant source of energy in the shadow zone.

1. Measurements With The CW Source

Figure 4 shows three raytracings for track 1 which were computed using the average sound-speed profile from the run and a source depth of 18 m. Each raytracing illustrates a different source position with respect to the seamount: a range from the receiver of 79 km in case A; 99 km in case B; and 119 km in case C. All bottom-bounce rays are omitted from the raytracings for clarity. For cases A and C, maximum shadowing is expected because the source is in a position which enables the seamount to intercept all of the deep refracted rays. In the absence of the seamount, these deep refracted rays
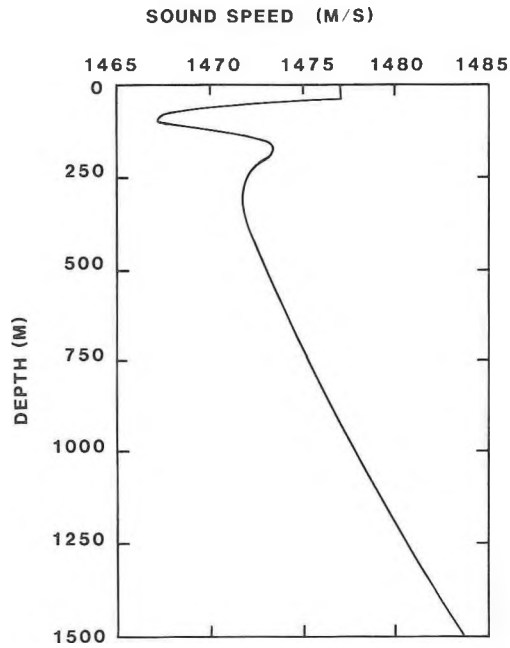
SOUND SPEED (M/S)

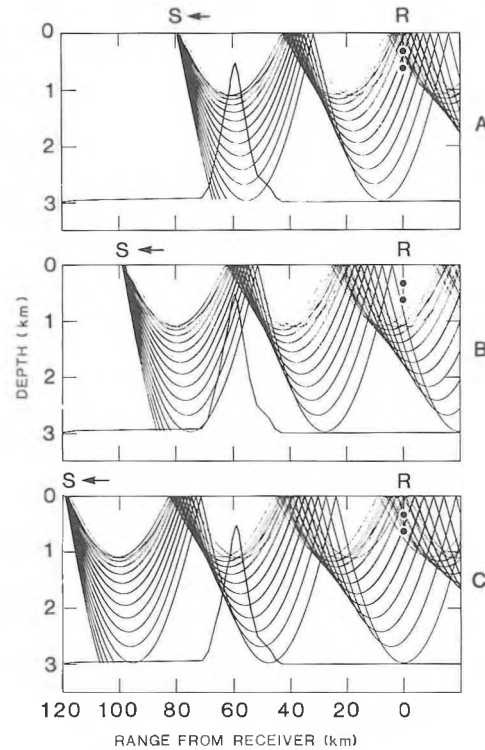Figure 3. Average sound-speed profile from all profile measurements.

Figure 4. Raytracings for radial track 1; source depth 18 m and source angles -15° to 15° in 1 degree increments. Receiver depths of 329 and 633 m are indicated by dots. The profile of the seamount is shown for three ranges: 79, 99, and 119 km.

would form a convergence zone at the receiver. For case B, the seamount intercepts only a small number of the deep refracted rays, so little shadowing should be seen.

Figure 5 contains the propagation loss results that were measured across the seamount (track 1) and over a flat bottom (track 2). In each case the cw source depth was 18 m, the receiver depth was 329 m, and the averaging time was 3.8 min. The smooth curve in Figure 5(a) is a propagation loss prediction from the FACT (Fast Asymptotic Coherent Transmission) ray model[10] with semicoherent addition. The prediction is based on the average sound-speed profile for track 1 and a flat bottom (as is assumed by FACT) with a FNWC (Fleet Numerical Weather Central) bottom loss classification type 2.[10] For the first 60 km, the measured results agree well with the predicted losses, particularly in the first bottom-bounce region (10-35 km) and in the first convergence zone (35-45 km). The peak (propagation loss minimum) between 57 and 60 km is an enhancement effect which is the result of acoustic reflection from the seamount and is discussed later in the paper. At ranges beyond 60 km, the point at which the source passed over the seamount, there is a marked increase in propagation loss caused by the shadowing effect of the seamount. In Figure 5(b), A, B, and C are the source ranges for the raytracings shown in Figure 4. As indicated by the raytracings, the results that were measured over the seamount (track 1) show maximum shadowing at A and C. For these ranges, the increase in propagation loss over the convergence zone level measured over the flat bottom (track 2) is about 15 dB. There is no similar increase in propagation loss at B, indicating the lack of interaction of the sound energy with the seamount.
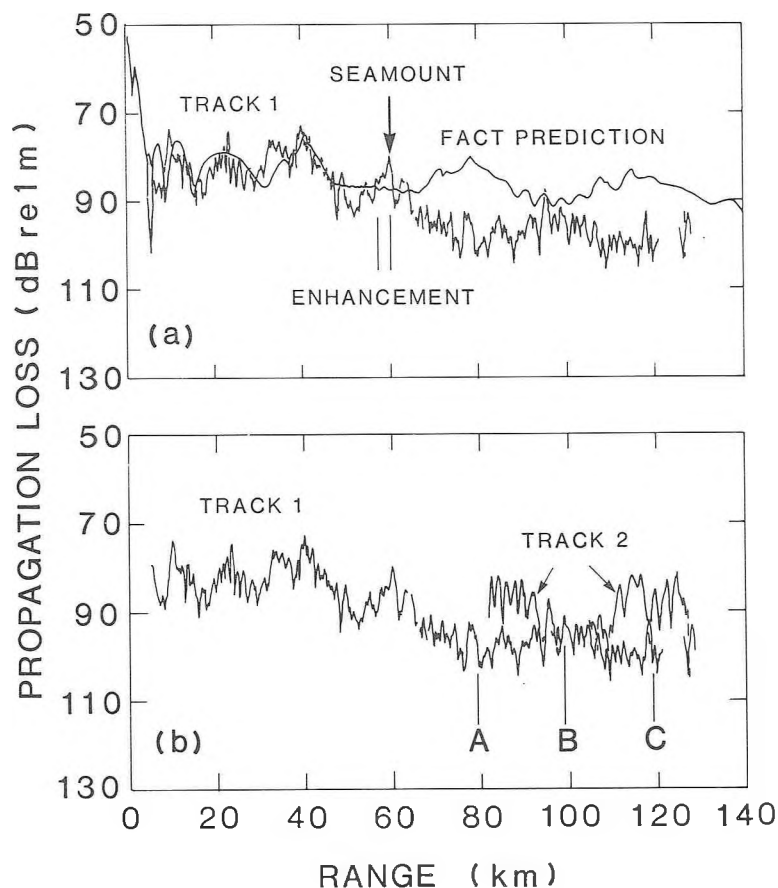
6

Figure 5. Measured propagation loss results for tracks 1 and 2; source depth 18 m and receiver depth 329 m. The smooth curve is a FACT model prediction based on a flat bottom. A, B, and C are the source ranges for the raytracings of Figure 4.

2. Ray Model Investigation Of Shadowing

The GRASS (Germinating Ray-Acoustics Simulation System) model,[11] which is capable of modelling range-dependent environments, was used to determine the bottom-surface propagation paths over the seamount with the cw source in positions A and C of Figure 4. These calculations used a source depth of 18 m and the average sound-speed profile and seamount bathymetry for track 1.

The investigation revealed that there are several possible ray paths over the seamount. These paths fall into one of three groups, depending upon the mode of propagation from the seamount to the receiver: (1) continuously refracted (RR) propagation; (2) refracted surface-reflected (RSR) propagation; and (3) bottom-bounce (BB) propagation. For cases A and C, the dominant arrivals at the receiver are RR arrivals which undergo one upslope reflection (1 USR) and one downslope reflection (1 DSR) on the seamount before propagating to the receiver. Secondary arrivals consist of RSR, BB and other RR arrivals with more seamount reflections. Figure 6 contains a raytracing which shows the dominant and secondary RR arrivals for case A. The dominant arrivals originate with source angles (measured from the horizontal) of 2.8°, 3.0° and 3.2° while the secondary arrival has a source angle of 4.4°. All of the arrivals in cases A and C originate as deep refracted rays with source angles of less than 12°. Virtually all of the rays with greater source angles are blocked by the seamount. It was found that for each of the RR and RSR arrivals predicted by the GRASS model, the grazing angles on the seamount for the first and last reflections are both less than the 17° critical angle of the assumed FNWC type 2 bottom loss. Thus the model introduces zero loss at these interactions. However, for the intermediate reflections the grazing
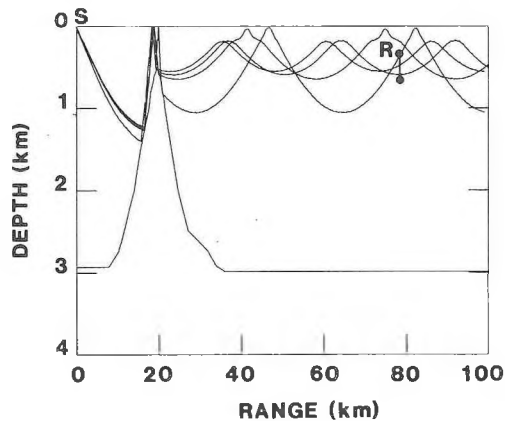
7

Figure 6. Raytracing showing the dominant (source angles 2.8°, 3.0° and 3.2°) and secondary (source angle 4.4°) RR arrivals for track 1, case A; source depth 18 m. Receiver depths of 329 and 633 m are indicated by dots.

angles generally range from 36° to 57°, well above the critical angle, thus introducing losses in the order of 6 to 9 dB per bottom reflection. This has the effect of reducing the significance of those paths that experience more than two reflections on the seamount. However, the GRASS model predicts that for cases A and C, there is at least one significant arrival (eigenray) that propagates to the receiver in the shadow zone with minimal interaction with the seamount (1 USR and 1 DSR), thus limiting the increase in propagation loss to the 15 dB observed in Figure 5.

3. Measurements With The Explosive Charges

The propagation loss results for track 5 are shown in Figure 7 for the 1/3 octave bands from 12.5 to 400 Hz. The shots were detonated at a depth of 24 m and the receiver was at a depth of 363 m. The bathymetry along the track is shown at the bottom of the figure. As was seen in the cw results, the seamount shadowing effect is evident from about 65 km, where the propagation loss increases abruptly, to about 95 km and from about 105 km out to the end of the run.

An example of the multipath arrival series measured at a source range of 79 km (case A of Figure 4) is shown in Figure 8, again for the 1/3 octave bands from 12.5 to 400 Hz. The pressure-time histories plotted in this figure are typical of those observed throughout most of the primary shadowing region between 65 and 95 km. At frequencies greater than 50 Hz, there are two significant arrivals, separated by about 0.5-0.8 s. The first arrival is a sharp pulse of width about 0.3 s, and is followed by a second arrival, or group of arrivals, which slowly decrease in magnitude over about 2 s. At this range, measurement of the multipath propagation loss indicated that the loss for the dominant first arrival was 6-10 dB less than the loss for the subsequent arrivals. At frequencies lower than 50 Hz, the behavior is significantly different, as the strong first pulse is not observed.

4. Diffraction Theory Interpretation Of Shadowing

The first arrival observed for the shots deployed at a source range of 79 km (Figure 8) is most likely a pulse propagating over the seamount by diffraction. Following the diffracted arrival is a group of arrivals propagating over the seamount by a number of bottom-surface reflections as predicted by ray theory. This identification of the acoustic paths was
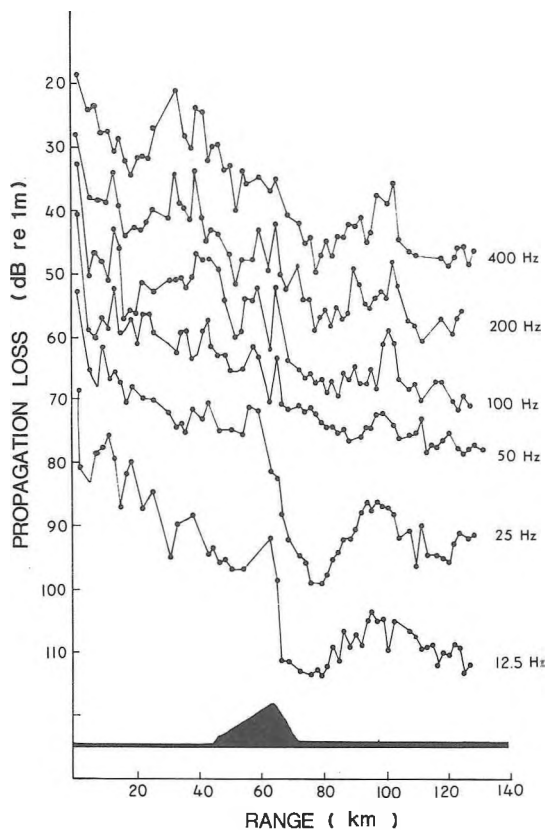
Figure 7. Propagation loss versus range from
the receiver for the 24-m shots of track 5.
The measurements are in 1/3-octave bands from
12.5 to 400 Hz and are offset by 10 dB. The
location and shape of Dickins Seamount is
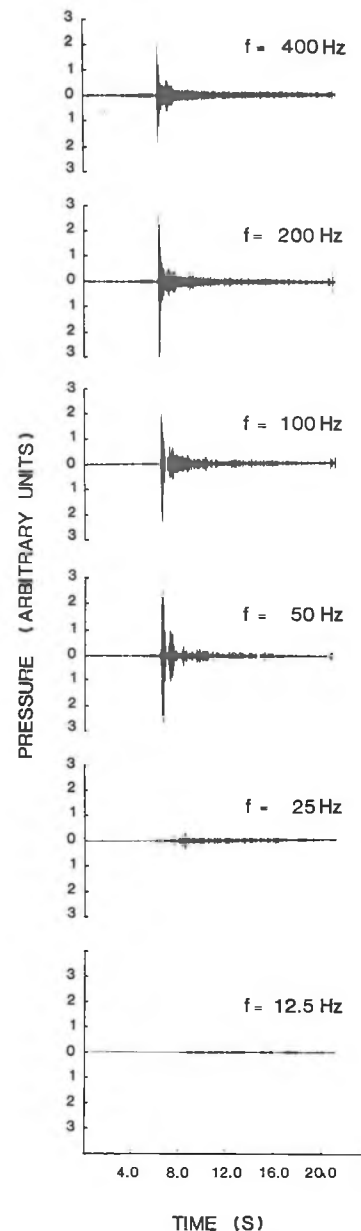shown at the bottom of the figure.

Figure 8. Pressure-time histories of a 24-m shot within the primary shadow
region at a range of 79 km from the receiver along track 5. The signals have
been filtered in 1/3-octave bands from 12.5 to 400 Hz.

determined by comparing the travel time of the first arrival within the shadow
zone (range 79 km) with that computed by ray theory predictions with the GRASS
model. The model predictions represent the earliest possible arrival times of
sound propagating over the seamount by bottom-surface reflections. In the
shadowing region, the ray theory predictions lagged the measured times by
0.5-1.0 s, roughly the arrival time difference observed in the data of Figure
8. A similar comparison was made at a source range of 100 km (outside the
shadow zone). Here ray theory predictions coincided with the measured time
since at this range the eigenrays did not interact with the seamount.

It is difficult to predict the travel time of the diffracted arrival
because there is no ray-path analog for the diffraction process. However, a
calculation was made for an equivalent ray path based on a model introduced by
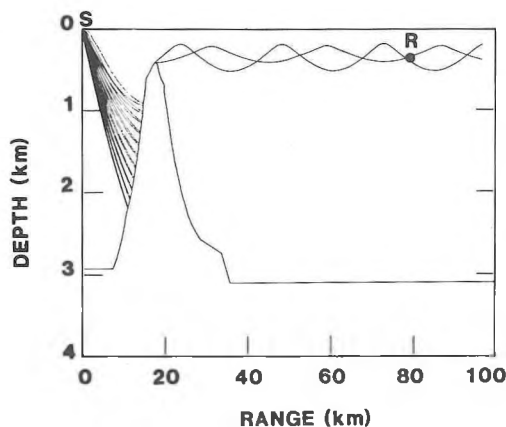
9

Figure 9. Raytracing showing
the equivalent ray path of the
diffracted wave for track 5,
case A; source depth 24 m,
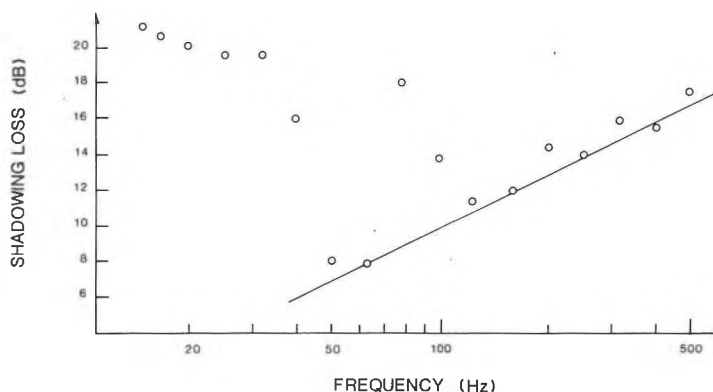receiver depth 363 m.

Figure 10. Shadowing loss for the track 5
24-m shots at an average range of 79 km.
The solid line is a plot of the diffraction
model prediction from reference 12.

Medwin et al.[12] The equivalent ray path of the model is shown in the
raytracing of Figure 9. The model includes the theory of diffraction over a
wedge and the results of laboratory experiments with a scale model of Dickins
Seamount combined with a ray model of propagation. Wave theory corrections
are included to model both the upslope propagation to the seamount peak by
forward scattering from the rough surface of the seamount and the
three-dimensional diffraction over the peak. For the travel time prediction
of the diffracted arrival, ray theory was used to calculate the travel time
from the source to the seamount, and from the seamount peak to the receiver.
The time taken to reach the seamount peak by forward scattering up the slope
was calculated using average sound-speeds over 100-m depth segments. The
predicted total travel time for the range of 79 km was 54 s, in close
agreement with the measured value of 53.5 s.

    The shadowing loss, which is loosely defined as the increased loss caused
by the interaction with the seamount over that expected in the absence of the
seamount, was computed for the results of Figure 7 by subtracting the FACT
model predictions for the loss over a flat bottom from the measured data. The
result was the average shadowing loss as a function of frequency for the range
interval 77-82 km as shown in Figure 10. Assuming that the dominant
contribution is due to the diffracted arrival, the diffraction model of Medwin
et al.[12] predicts an $f^{1/2}$ dependence for the shadowing loss. This prediction,
shown by the solid line, is in good agreement with the measured results for
frequencies greater than 50 Hz, but fails to model the results obtained at
lower frequencies. It is possible that the increase in shadowing loss at low
frequencies is due to surface-decoupling which causes an increase in the
propagation loss for shallow sources.[13,14] However, the disagreement at low
frequencies could also be caused by a change in the scattering behavior from
rough-surface forward scattering (for f > 50 Hz) to smooth-surface specular
reflection (for f < 50 Hz). If the seamount slope is effectively smooth for
low frequencies, only the arrival predicted by ray theory would propagate over
the seamount. There is some support for this hypothesis in the multipath
arrival histories measured in the primary shadow region. As shown in Figure
8, the strong diffracted arrival is not observed at frequencies below 50 Hz.

10

ACOUSTIC REFLECTIONS FROM THE SEAMOUNT

During the propagation loss experiments, when either the shallow cw or shallow explosive sources were on the same side of the seamount as the receiver and within 15 km of the seamount peak, reflections from the seamount were found to be significant. These reflections appeared over the entire range of receiver depths (329-633 m). Ray theory predicts that the reflections were a result of the seamount redirecting the source energy through a series of bottom-surface reflections up and then down the seamount side.

1. Measured Reflections

Figure 11 shows a series of time-averaged spectra for the portion of track 1 when the cw source approached to within 10 km of the seamount peak. The receiver depth was 329 m and the length of each average was 3.8 min, corresponding to a range interval of 0.68 km. The direct arrival[15] in the spectra has a down-Doppler frequency shift because the source ship was opening range from the receiver. Because the source was closing range on the seamount, the seamount-reflected arrivals have up-Doppler shifts.

In these results, the Doppler-shifted direct arrival is dominant in level and stable in frequency throughout the 10-km range interval. Raytracings based on the average sound-speed profile and measured bathymetry of track 1 indicate that the energy of the direct arrival originated from the source at an angle of about 16° and propagated to the receiver via second bottom-bounce paths. The measured Doppler shift of the direct arrival, which can be related to the source angle through ship speed and the sound-speed at the source, also indicates an angle of about 16°. There are two reflected arrivals with

Figure 12. Raytracing illustrating the reflection process with the source 6 km from the seamount peak along track 1; source depth 18 m and source angles 15°, 124°, 132.5°, and 158°.
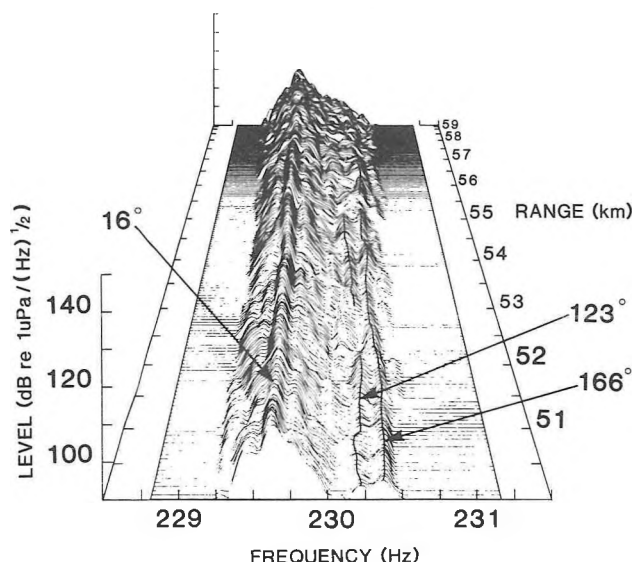
Figure 11. Variation of the measured spectral results with range for track 1; source ranges 50 to 60 km, source depth 18 m, and receiver depth 329 m. The seamount peak was at a range of 60 km. The arrival labelled 16° is the direct arrival while the 123° and 166° arrivals are arrivals reflected back from the seamount.
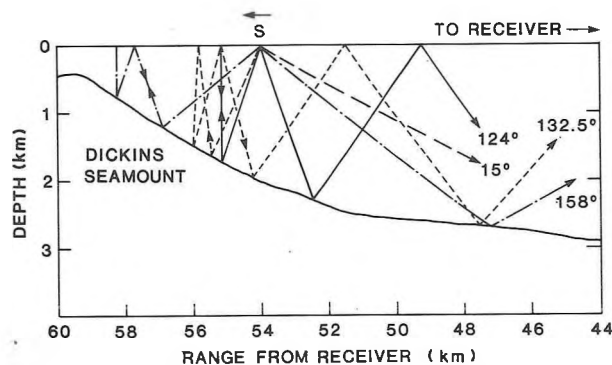
distinctly different Doppler-shifts evident in the first 5 km of the figure. Both reflected arrivals are relatively stable in frequency over that range interval and their Doppler shifts indicate that the source angles from which they originated were about 166° for the dominant arrival and about 123° for the secondary arrival. The difference in level between the dominant reflected arrival and the direct arrival averages about 14 dB over the 5-km interval with a minimum difference of 6 dB at a source range of 56 km (measured when the source was 4 km from the seamount peak).

2. Ray Model Investigation Of Reflection

The GRASS model was used to investigate the reflection mechanism using the same environment and geometry as that for the study of seamount shadowing. Figure 12 shows a raytracing with a source range of 54 km (6 km from the seamount peak). The angles in the figure are the source angles of the eigenrays. Of all the energy insonifying the seamount, only that energy represented by the reflected rays of this figure propagates to the receiver.

The 158° ray is the dominant reflected arrival. It undergoes 2 USR and 2 DSR before propagating to the receiver via a 3-BB path. The secondary arrival from 124° undergoes 1 USR, 2 DSR, and 4 BB before reaching the receiver. The 15° ray is the dominant direct arrival and undergoes 2 BB while propagating to the receiver. These three arrivals are close enough in source angle to those seen in the measured results of Figure 11 to indicate that the dominant reflected paths have been identified. Similar results were found when the ray investigation was carried out at source ranges of 53, 55, and 56 km.

ACOUSTIC ENHANCEMENT BY THE SEAMOUNT

It was found during the propagation loss experiments that when either the shallow cw or shallow explosive sources were nearly over the seamount peak, an appreciable signal enhancement of the direct arrival was produced. This enhancement was observed over the entire range of receiver depths (329-633 m). The cw measurements indicated that during this enhancement the reflected arrival had nearly the same Doppler shift as the direct arrival. Ray theory predicts that the direct arrival was enhanced with energy that was converted via downslope reflection on the seamount to RSR paths.

1. Measured Enhancement

Figure 13 contains the time-averaged spectra for the last 4 km of data displayed in Figure 11. At source ranges beyond 57 km, the direct arrival in the down-Doppler region is paired with a second arrival which has a slightly smaller down-Doppler shift. The magnitude of that shift indicates that the new arrival originated from the source at an angle of about 40°. It appears that as the source approached to within 3 km of the seamount peak, the reflected path shifted to that of a single DSR arrival which originated with a source angle of about 40°. The results shown in the figure also indicate that as the source approached to within 1 km of the peak, the reflected arrival became inseparable from the direct arrival. This resulted in an enhancement of the direct arrival that was responsible for the 10-dB decrease in the propagation loss at 60 km as shown in Figure 5.
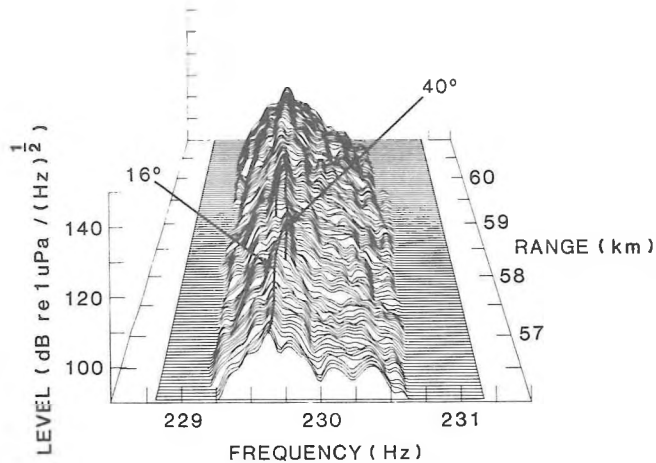
12

Figure 13. Variation of the measured spectral results with range for track 1; source ranges 56 to 61 km, source depth 18 m, and receiver depth 329 m. The seamount peak was at a range of 60 km. The 16° arrival is the direct, while the 40° arrival was reflected from the seamount.
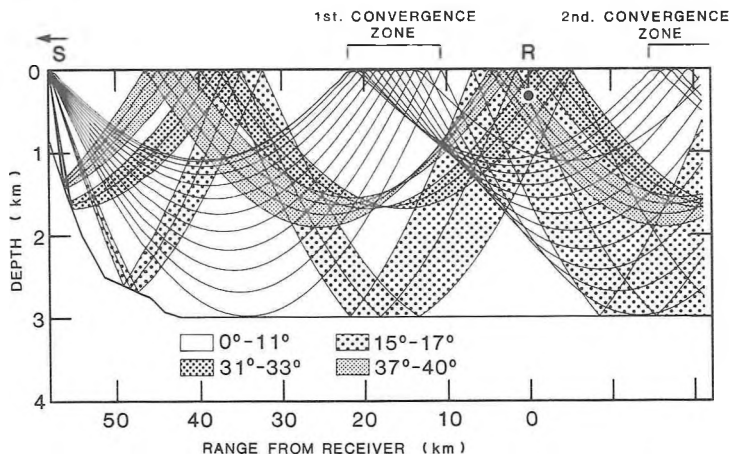

Figure 14. Raytracing illustrating the enhancement process with the source 2 km from the seamount peak along track 1; source depth 18 m, receiver depth 329 m, and source ray fans 0° to 11°, 15° to 17°, 31° to 33°, and 37° to 40° in 1 degree increments.

2. Ray Model Investigation Of Enhancement

The GRASS model was used to determine the mechanism which was responsible for the enhancement of the direct arrival using the same conditions as in the previous studies. Figure 14 shows a raytracing which illustrates the enhancement process at a source range of 58 km (2 km from the seamount peak). Four ray fans are plotted: the 0° to 11° fan which forms the convergence zones; the 15° to 17° fan which forms the second bottom-bounce arrival at the receiver; the 31° to 33° fan; and the 37° to 40° fan. The latter two ray fans form two convergent arrivals, each of which surface in the same region as the second bottom-bounce arrival. As the raytracing illustrates, the second bottom-bounce signal (direct arrival) is enhanced with energy that reflects (DSR) from the side of the seamount and then propagates along RSR paths to the receiver. The arrivals illustrated in this raytracing compare well in source angles with those calculated from the Doppler shifts observed in Figure 13 thus suggesting that the propagation paths of the enhancing arrivals have been correctly identified. Similar results were found when the ray investigation was carried out at source ranges of 57, 59, and 60 km. In agreement with the measured results of Figure 5, no enhancement effect is predicted for the ranges beyond 60 km, the point at which the source passes over the seamount peak.

RESULTS FOR THE DEEP SOURCES

The propagation loss results for the deep sources indicated that the seamount did not present as significant a barrier to sound propagation as for the shallow sources. Because the energy from the deep sources was confined more closely to the sound-channel axis, most of the sound propagated over the peak without interacting with the seamount. Consequently, the shadowing effect was greatly reduced and the source energy that propagated along the channel axis masked out any of the reflected or enhancing arrivals that might have been present.

CONCLUSIONS

These experiments have provided a reasonably detailed accounting of the acoustic interaction of low-frequency sound with Dickins Seamount, a relatively isolated bathymetric feature located off the Canadian west coast. The investigation revealed three types of acoustic interactions: shadowing; reflection; and downslope enhancement. The occurrence of these interactions and their effects on the propagation loss measured at a receiver located 60 km from the seamount were found to depend on both the depth and position of the source relative to the seamount and receiver.

When the source was shallow and in a position on the opposite side of the seamount from the receiver, such that the seamount intercepted the deep refracted energy, an acoustic shadow was cast over the receiver. Within this shadow, the propagation loss to the receiver increased by up to 15 dB over the convergence zone level measured over an area with a flat bottom. An examination of the multipath propagation loss results revealed that the source energy received in the shadow zone was composed of two arrivals. The first and dominant arrival resulted from deep refracted energy that was forward-scattered by the rough surface of the seamount slope and then diffracted over the peak. This was followed by a group of secondary arrivals composed of deep refracted energy that propagated over the seamount by a number of bottom-surface reflections up and then down the slope. However, for frequencies less than 50 Hz, only the reflected arrivals were observed. It is speculated that this was caused by a change in the scattering mechanism from rough-surface forward scattering at high frequencies to smooth-surface specular reflection at low frequencies. These results are supported by a diffraction model of seamount shadowing introduced by Medwin et al.[12]

When the shallow cw source approached the seamount to within 10 km from the same side as the receiver, acoustic energy was reflected from the seamount back to the receiver. Because of the Doppler shift created by the moving source, these reflections were separable in frequency from the directly received energy. A ray model investigation indicated that the reflections were the result of the seamount redirecting the source energy though a series of bottom-surface reflections up and then down the seamount side. It was found that the number of reflections required to turn the energy was a function of the angle at which the energy left the source. At closer ranges, when the source was within 3 km of the seamount peak, a portion of the source energy underwent a single downslope reflection from the seamount slope before being launched onto an RSR path to the receiver. Because this reflected arrival had essentially the same Doppler shift as the directly received energy, it was inseparable from it, and an enhancement of the direct arrival at the receiver resulted.

REFERENCES

1. G.R. Ebbeson and R.G. Turner, "Sound Propagation Over Dickins Seamount in the Northeast Pacific Ocean", J. Acoust. Soc. Am. 73, 143-152 (1983).

2. N.R. Chapman and G.R. Ebbeson, "Acoustic Shadowing by an Isolated Seamount", J. Acoust. Soc. Am. 73, 1979-1984 (1983).

3. J. Northrop, "Underwater Sound Propagation Across the Hawaiian Arch", J. Acoust. Soc. Am. 48, 417-418 (1970).

4. R.W. Bannister, D.G. Browning, and R.N. Denham, "The Effect of Seamounts on SOFAR Channel Propagation", J. Acoust. Soc. Am. 55, 417 (1974).

5. G.B. Morris, "Preliminary Results on Seamount and Continental Slope Reflection Enhancement of Shipping Noise", Marine Physical Laboratory Report No. U-57/75, Scripps Institution of Oceanography, San Diego, CA (November 1975).

6. R.W. Bannister, R.N. Denham, K.M. Guthrie, and D.G. Browning, "Project TASMAN TWO: Low-frequency Propagation Measurements in the South Tasman Sea", J. Acoust. Soc. Am. 62, 847-859 (1977).

7. D.A. Nutile and A.N. Guthrie, "Acoustic Shadowing by Seamounts", J. Acoust. Soc. Am. 66, 1813-1817 (1979).

8. K.M. Guthrie, R.N. Denham, R.W. Bannister, and D.G. Browning, "Models for Acoustic Propagation over a Seamount of the Louisville Ridge", J. Acoust. Soc. Am. Suppl. 1 69, S58 (1981).

9. R.N. Denham, R.W. Bannister, K.M.Guthrie, and D.G. Browning, "Low-frequency Sound Propagation in the South Fiji Basin", J. Acoust. Soc. Am. 75, 406-412 (1984).

10. C.W. Spofford, "The FACT Model", Vol. I, Maury Center Report No. 109, Acoustic Environmental Support Detachment, Office of Naval Research, Arlington, VA (November 1974).

11. J.J. Cornyn, "GRASS: A Digital-Computer Ray-Tracing and Transmission-Loss-Prediction System, Volume 1 - Overall Description", Naval Research Laboratory Report No. 7621, Washington, DC (December 1973).

12. H. Medwin, E. Childs, E.A. Jordan and R.A. Spaulding, "Sound Scatter and Shadowing at a Seamount: Hybrid Physical Solutions in Two and Three Dimensions", J. Acoust. Soc. Am. 75, 1478-1490 (1984).

13. R.W. Bannister and M.A. Pedersen, "Low Frequency Surface Interference Effects in Long Range Sound Propagation", J. Acoust. Soc. Am. 69, 76-83 (1981).

14. F.B. Jensen, "Sound Propagation over a Seamount", presented at the 11th, International Conference on Acoustics (I.C.A.), Paris, France, July 1983.

15. In the context of this paper, a direct arrival is any arrival which reaches the receiver without interacting with the seamount.